On 1-D PDE-Based Cardiovascular Flow Bottleneck Modeling and Analysis: A Vehicular Traffic Flow-Inspired Approach

Nikolaos Bekiaris-Liberis, *Member, IEEE*

***Abstract*—We illustrate the potential of partial differential equation (PDE)-based traffic flow control in cardiovascular flow analysis, monitoring, and control, presenting a PDE-based control-oriented formulation, for one-dimensional (1-D) blood flow dynamics in the presence of stenosis. This is achieved adopting an approach for modeling and analysis that relies on the potential correspondence of 1-D blood flow dynamics in the presence of stenosis, with 1-D traffic flow dynamics in the presence of bottleneck. We reveal such correspondence in relation to the respective (for the two flow types), speed dynamics and a (consistent with them) fundamental diagram-based reduction; bottleneck dynamic effects description and resulting boundary conditions; and free-flow/congested regimes characterization.**

***Index Terms*—Cardiovascular flow stenosis, hyperbolic PDE systems, modeling, traffic flow bottleneck.**

I. Introduction

Arterial stenosis, due to, for example, atherosclerotic plaque building up in arteries or in-stent restenosis, is a primary cause of human losses worldwide [13]. A great number of deceases, attributed to congested blood flow, currently accounting for about 50% of deaths within the European Union [34], could be avoided with accurate/timely detection and action implementation. This is true particularly in view of the practical feasibility that is supported by existing technologies, such as smart, stents and bypass grafts, and other implantable or noninvasive devices, where actuation and sensing may be performed wirelessly, via communication with a central computer; see, e.g., [8], [12], [13], [26], [49], [50].

Despite the technological advancement and urgent need for availability of respective advanced methodologies, illustrated by their potential in congested blood flow detection/treatment, there exists no *control-theoretic* approach tackling the formulation, analysis, monitoring, and feedback control problems of congested blood flow, in its natural, continuous in time/space, domain, in the presence of stenosis. However (and despite the domain and dimensional complexity of cardiovascular flow), there exist one-dimensional(1-D), second-order, hyperbolic partial differential equation (PDE) systems that may effectively describe (on average) blood flow dynamics; see, e.g., [11], [19], [21], [30], [35], [46]. Thus, such models may be utilized as basis for control-theoretic modeling, analysis, and design purposes.

In this article, we launch an effort in this direction formulating and analyzing, from a *PDE-based traffic flow control* (see, e.g., [10], [15], [17], [22], [24], [33], [44], [45], [56], [58]) perspective, the dynamics of 1-D blood flow in the presence of stenosis. The stenosis is considered to be located at the boundary of the arterial segment considered. We present two alternative formulations in which the stenosis dynamics are characterized via a static or dynamic description for the pressure drop through the stenosis. Together with utilization of a baseline dynamic model for blood flow, capturing the main transport phenomena and respective mass/momentum conservation principles, such formulation gives rise to a 2×2 (heterodirectional; see, e.g., [3], [23]) hyperbolic PDE system, with a static or dynamic boundary condition, at the outlet of the artery segment considered, respectively. As the location, geometry, and length of the potential stenosis are considered to be unknown, the derived model may incorporate unknown PDE domain length and boundary conditions parameters. We recast the problems of real-time blood flow estimation and stenosis characteristics (in particular, stenosis' location, length, and section area) identification as problems of state estimation and parameters identification of a class of 2×2 hyperbolic PDE systems with uncertain characteristic speeds and boundary parameters, which have not been formulated elsewhere.

For the derived dynamic descriptions of 1-D blood flow in the presence of stenosis, we then illustrate the correspondence of certain features with traffic flow dynamics in the presence of bottleneck. We explore correspondence with Payne–Whitham- and Aw–Rascle–Zhang-type models, in particular, in relation to speed dynamics and a consistent (with respect to reduction to conservation law equation, for instance, of Lighthill–Whitham–Richards-type) fundamental diagram. Furthermore, we illustrate the connection to respective, dynamic models of traffic flow bottlenecks. In particular, boundary blood flow stenosis may be characterized via the pressure drop at the stenosis location, while boundary traffic flow bottleneck may be described via the capacity drop at the bottleneck area. Moreover, for each type of stenosis description, we provide a consistent boundary condition at the outlet, which could either be static or dynamic, also illustrating the correspondence with the respective boundary conditions, in the case of traffic flow bottleneck. We also discuss the analogy between characterization of free-flow/congested traffic regimes and supercritical/subcritical blood flow regimes. Consistent simulation results are provided for the two boundary stenosis' descriptions. Illustration of the fact that the two different applications, namely, cardiovascular and traffic systems, could be treated utilizing techniques from a common theme, despite the fact that the underlying dynamic phenomena, giving rise to blood and traffic flow are fundamentally different, is significant and it has not been illustrated elsewhere in literature.

The rest of this article is organized as follows. In Section II, we present a control-oriented model for blood flow in which arterial stenosis is described either as static or dynamic, boundary bottleneck. In Section III, we analyze the obtained hyperbolic system, revealing the dynamic correspondence with traffic flow dynamics in the presence of bottlenecks. In Section IV, we present simulation results and discuss how the models presented can be utilized for adaptive observer design. Finally, Section V concludes this article.

Manuscript received 30 May 2022; accepted 23 July 2022. Date of publication 29 July 2022; date of current version 29 May 2023. This work was supported by the Hellenic Foundation for Research and Innovation (H.F.R.I.) under Project 3537/ORAMA. Recommended by Associate Editor Y. Le Gorrec.

The author is with the Department of Electrical and Computer Engineering, Technical University of Crete, 73100 Chania, Greece (e-mail: bekiaris-liberis@ece.tuc.gr).

Color versions of one or more figures in this article are available at https://doi.org/10.1109/TAC.2022.3195148.

Digital Object Identifier 10.1109/TAC.2022.3195148

II. Control-Theoretic Modeling of Stenosis

A. 1-D Cardiovascular Flow Model

We consider the following 2×2 hyperbolic system, which constitutes an 1-D approximation of cardiovascular flow dynamics (see, e.g., [19], [21], [35]):

$$A_t(x,t) = -A_x(x,t)V(x,t) - A(x,t)V_x(x,t) \tag{1}$$

$$V_t(x,t) = -V(x,t)V_x(x,t) - \frac{1}{\rho}P_x\left(A(x,t)\right) - K_r\frac{V(x,t)}{A(x,t)} \tag{2}$$

$$A(0,t)V(0,t) = Q_{\text{in}}(t) \tag{3}$$

where $A > 0$ is the section area of the artery, $V > 0$ is the average blood speed, $\rho > 0$ is the blood density, $K_r > 0$ is the friction parameter related to blood viscosity, $t \geq 0$ is the time, $x \in [0, D]$ is the spatial variable, $D > 0$ is the length of the artery segment considered, $P \in \mathbb{R}$ is the pressure, which accounts for vessel wall displacement, and $Q_{\text{in}} > 0$ the is flow at the inlet of the artery segment considered (it could, e.g., be described by a periodic signal, with period equal to the cardiac cycle, see, e.g., [35]). A possible expression for the pressure function is (see, e.g., [21], [35])

$$P(A) = \frac{\beta}{A_0}\left(\sqrt{A} - \sqrt{A_0}\right) \tag{4}$$

$$\beta = hE\sqrt{\pi}b \tag{5}$$

where A_0 is the reference arterial section area at rest, $h > 0$ is the artery wall thickness, $E > 0$ is Young's modulus, and b is a positive parameter. One boundary condition, associated with (1) and (2), is provided in (3), describing the blood flow entering the arterial segment considered. The second boundary condition is specified in the following sections since it depends both on the sign of the eigenvalues of hyperbolic system (1), (2) as well as the stenosis dynamic description adopted.

In this setup, in which the case of a boundary bottleneck is considered, it is assumed that parameters β and A_0, in the pressure equation (4), are known and constant throughout the domain, which may be a reasonable requirement given that variations in geometry and mechanical properties of the artery, imposed by the stenosis, are considered to be located at the boundary $x = D$. Although most of modeling and analysis developments could be performed considering spatially varying coefficients β and A_0, for presentation and formulation simplicity, as well as to not distract the reader from the main scope of this article, which is presentation and analysis of a control-theoretic, stenosis model and its correspondence with traffic flow bottleneck model, we do not consider this case here.

B. Formulation of Available Measurements Output Equation

In this article, we consider the case in which the pressure and flow at the inlet of the artery segment considered are measured in real time. Although such a setup may appear, at first sight, as unrealistic, current technological advancements enable the availability of these measurements. In particular, such measurements could be wirelessly transmitted to a central computer, utilizing smart stent (or other implantable) devices, see, for example, [13], [26], [39], [50], as well as noninvasive devices, see, e.g., [8], [49]. Thus, besides having available Q_{in}, a measured output is available, given by

$$y(t) = P\left(A(0,t)\right). \tag{6}$$

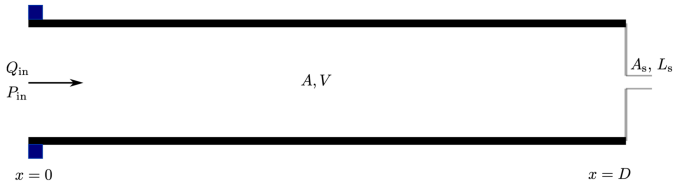

Fig. 1. Simplified schematic of an 1-D approximation of an arterial segment at rest with boundary stenosis. At the inlet of the segment considered (i.e., for $x = 0$), an implantable smart stent device measures pressure and flow (i.e., P_{in} and Q_{in}, respectively). The bottleneck location D, stenosis cross-sectional area A_{s}, and stenosis length L_{s} may be unknown.

Since location, geometry, and material properties of the stent, in realistic scenarios, could be considered as known, it follows that β and A_0 at $x = 0$ are known (even in the case in which β and A_0 may take different values, as compared with their values for $x \in (0, D)$). Thus, using (4), measurements of $A(0,t)$ could be obtained, and hence, using (3), measurements of $V(0,t)$.

Inflow Q_{in} could be viewed in two different ways. One is as an exogenous, nevertheless, measured input, which is realistic from a practical viewpoint. For this reason, we focus in this article on the formulation and analysis of a blood flow model in the presence of stenosis, which may be suitable for solving the state estimation and parameters identification problems (see also Section IV-B). The other is viewing Q_{in} as manipulated input. Even though it may be currently technologically difficult to manipulate blood flow at a specific point, there is enough evidence that such implementations could become feasible in the future. In particular, current technological advances, such as smart shunts [41] (able to manipulate artery radius via communication with a computer), suggest that such implementations may indeed become possible.

C. Stenosis Model as Static Boundary Bottleneck

This potential formulation of a bottleneck is derived assuming that the stenosis (e.g., due to atherosclerotic plaque building up at arterial wall [34] or in-stent restenosis [13]) is located downstream of the inlet (i.e., the known location of a, for instance, stent device). In particular, we treat the right boundary of the arterial segment considered as the point at which the potential stenosis is located. Therefore, x belongs to $[0, D]$, where D may be unknown as the stenosis location may be unknown. The right boundary condition is derived such that it incorporates the effect of stenosis in the outlet. A schematic view of the setup considered is shown in Fig. 1.

1) Modeling Assumptions: In this setup, the domain length D and the effective section area at the stenosis location A_{s} may be unknown.[1] In particular, the stenosis section area is assumed to be constant, which may be a reasonable assumption given the material and elastic properties of atherosclerotic plaque (see, e.g., [40]). It is further assumed that (for constant A_{s}) flow is conserved through the stenosis. Moreover, the least complex formulation of the stenosis effect (at least in terms of the number of potentially unknown model parameters) could be obtained assuming (initially) zero (or, effectively, very small) length for the stenosis.

2) Boundary Condition Formulation: Consequently, at the stenosis location, the following relation may be satisfied ([36], [52],

[1]The stenosis may be assumed to be axisymmetric (see, e.g., [53]; see also, for instance, [29] and [32], for more complex, potential stenosis geometries).

[53]; see also [14], [27], [38] for relevant expressions):

$$\Delta P\left(A(D,t),V(D,t)\right)=V(D,t)^2\frac{K_{\mathrm{s}}\rho}{2}\left(\frac{A(D,t)}{A_{\mathrm{s}}}-1\right)^2 \quad (7)$$

where $\Delta P(A(D),V(D))$ denotes the pressure drop due to the stenosis, while parameter $K_{\mathrm{s}}>0$ is known (obtained, e.g., from experimental data, see, e.g., [36]). The pressure drop denotes the pressure difference between the locations before and after the stenosis. For the former, we may assume that it is given by (4), while for the latter, we may assume that it is described such that a terminal boundary condition, modeling the effect of blood flow dynamics in arteries downstream of the stenosis (see, e.g., [20], [38]), is imposed. Therefore, we may define

$$\Delta P\left(A(D,t),V(D,t)\right)=P\left(A(D,t)\right)-R_{\mathrm{T}}A(D,t)V(D,t) \quad (8)$$

with $Q_{\mathrm{s}}=A(D)V(D)$ denoting the flow at the inlet of the stenosis, where $R_{\mathrm{T}}\geq 0$ denotes a total, terminal resistance. Parameter R_{T} may be chosen depending on the blood flow conditions modeled for a considered arterial network, and thus, it may be considered as known. Using (4), (7), and (8), we obtain

$$\frac{\beta}{A_0}\left(\sqrt{A(D,t)}-\sqrt{A_0}\right)-R_{\mathrm{T}}A(D,t)V(D,t)$$
$$-V(D,t)^2\frac{K_{\mathrm{s}}\rho}{2}\left(\frac{A(D,t)}{A_{\mathrm{s}}}-1\right)^2=0. \quad (9)$$

Equation (9) prescribes a boundary condition at $x=D$, associated with system (1)–(3), with A_{s} and D being unknown.

Although, as starting point and under the assumption of zero stenosis length, formulation (9) may appear to be adequately realistic, a more accurate, nevertheless more complex, formulation for the right boundary condition (at the inlet of the stenosis) may be obtained utilizing the following relation for the pressure drop (see, e.g., [36], [52], [53]):

$$\Delta P\left(A(D,t),V(D,t)\right)=\frac{8\pi\mu L_{\mathrm{s}}}{A_{\mathrm{s}}^2}A(D,t)V(D,t)+V(D,t)^2$$
$$\times\frac{K_{\mathrm{s}}\rho}{2}\left(\frac{A(D,t)}{A_{\mathrm{s}}}-1\right)^2 \quad (10)$$

where $L_{\mathrm{s}}>0$ is the unknown stenosis length and μ is the known blood viscosity coefficient. Thus, using (4), (8), and (10), we obtain

$$\frac{\beta}{A_0}\left(\sqrt{A(D,t)}-\sqrt{A_0}\right)-\left(R_{\mathrm{T}}+\frac{8\pi\mu L_{\mathrm{s}}}{A_{\mathrm{s}}^2}\right)A(D,t)$$
$$\times V(D,t)-V(D,t)^2\frac{K_{\mathrm{s}}\rho}{2}\left(\frac{A(D,t)}{A_{\mathrm{s}}}-1\right)^2=0. \quad (11)$$

In the case of boundary condition (11), in addition to A_{s} and D, the stenosis length L_{s} may also be an unknown parameter.

D. Stenosis Model as Dynamic Boundary Bottleneck

Boundary condition formulations (9) and (11) may be accurate for zero or, effectively, very small, stenosis length. A potentially more realistic, nevertheless more complex, model of the pressure drop dynamics, accounting for larger stenosis length (yet, much smaller than the length D of the arterial segment considered), may be written as (see, e.g., [38], [53])

$$V_t(D,t)=\frac{1}{\rho L_{\mathrm{s}}}\Delta P\left(A(D,t),V(D,t)\right)-V(D,t)^2\frac{K_{\mathrm{s}}}{2L_{\mathrm{s}}}$$
$$\times\left(\frac{A(D,t)}{A_{\mathrm{s}}}-1\right)^2-\frac{8\pi\mu}{\rho A_{\mathrm{s}}^2}A(D,t)V(D,t). \quad (12)$$

Employing (4) and (8), relation (12) may be written as

$$V_t(D,t)=\frac{\beta}{\rho A_0 L_{\mathrm{s}}}\left(\sqrt{A(D,t)}-\sqrt{A_0}\right)-\left(\frac{A(D,t)}{A_{\mathrm{s}}}-1\right)^2$$
$$\times\frac{K_{\mathrm{s}}}{2L_{\mathrm{s}}}V(D,t)^2-\left(\frac{8\pi\mu}{\rho A_{\mathrm{s}}^2}+\frac{R_{\mathrm{T}}}{\rho L_{\mathrm{s}}}\right)A(D,t)V(D,t). \quad (13)$$

Complete model (1)–(3), (13) consists of a nonlinear hyperbolic PDE – nonlinear ordinary differential equation (ODE) coupled system. One could consider an ODE for the pressure dynamics downstream of stenosis (instead of relation $R_{\mathrm{T}}AV$ in (8), e.g., [38]). For formulation and presentation simplicity, we do not consider the stenosis pressure dynamics here.

The dynamic stenosis model is expected, in general, to be more accurate as it captures the dynamics of the inherently pulsatile (oscillating) blood flow as well as the pressure drop dynamics at the stenosis, see, for example, [53]. However, as first step and for simplicity of formulation (such that, e.g., the problems of state estimation and parameters identification become more tractable) one could employ the static stenosis model. From a more practical viewpoint, an a priori choice of the potential stenosis model could be made guided by practical considerations, such as depending on the artery and potential stenosis geometries, as well as on the pressure drop estimation accuracy required. In particular, the static boundary bottleneck model (9) [obtained from (12) assuming that the length of stenosis is negligible, compared to the length of the artery segment considered] could be employed, as the first step and for simplicity of formulation, for specifying a static boundary condition (viewing the stenosis as a single point), which involves only one unknown parameter namely, the section area of the stenosis (see also Section IV-B).

III. Analysis of the Cardiovascular Flow Model and Its Relation to Traffic Flow Dynamics

A. Analysis of the Hyperbolic System

1) Blood Flow Information Propagation: In physiological conditions blood flow is reported to lie in congested (or, subcritical) regime (see, e.g., [21], [35]). In particular, the eigenvalues of the hyperbolic system (1) and (2) are given by

$$\bar{\lambda}_1(A,V)=V+\sqrt{\frac{\beta}{2\rho A_0}}A^{\frac{1}{4}} \quad (14)$$

$$\bar{\lambda}_2(A,V)=V-\sqrt{\frac{\beta}{2\rho A_0}}A^{\frac{1}{4}}. \quad (15)$$

Since we are concerned with the case of subcritical regime, we restrict our attention in a nonempty, connected open subset Ω of the set $\bar{\Omega}=\{(A,V)\in\mathbb{R}^2:0<A,0<V\}$, such that $V<\sqrt{\frac{\beta}{2\rho A_0}}A^{\frac{1}{4}}$, and hence, $\bar{\lambda}_1>0$ and $\bar{\lambda}_2<0$, in the region of interest. System (1)–(3) is then strictly hyperbolic with distinct, real nonzero eigenvalues, as long as $(A,V)\in\Omega$, which implies that information propagates both forward (with blood flow) and backward (at a lower speed).

2) Transformation to Riemann Variables: The Riemann invariants that correspond to the hyperbolic system (1) and (2) with

eigenvalues (14) and (15) are defined as

$$u(A,V) = V + 2\sqrt{\frac{2\beta}{\rho A_0}}A^{\frac{1}{4}} \tag{16}$$

$$v(A,V) = V - 2\sqrt{\frac{2\beta}{\rho A_0}}A^{\frac{1}{4}}. \tag{17}$$

The inverse transformations that correspond to (16) and (17) are

$$V(u,v) = \frac{1}{2}(u+v) \tag{18}$$

$$A(u,v) = \frac{\rho^2 A_0^2}{4^5\beta^2}(u-v)^4. \tag{19}$$

In the new variables, system (1) and (2) is written as

$$\begin{aligned} u_t(x,t) = &-\lambda_1(u(x,t),v(x,t))\,u_x(x,t) \\ &+ f_1(u(x,t),v(x,t)) \end{aligned} \tag{20}$$

$$\begin{aligned} v_t(x,t) = &-\lambda_2(u(x,t),v(x,t))\,v_x(x,t) \\ &+ f_1(u(x,t),v(x,t)) \end{aligned} \tag{21}$$

where

$$\lambda_1(u,v) = \frac{5u+3v}{8} \tag{22}$$

$$\lambda_2(u,v) = \frac{3u+5v}{8} \tag{23}$$

$$f_1(u,v) = -\frac{4^{\frac{9}{2}}K_r\beta^2}{\rho^2 A_0^2}\frac{u+v}{(u-v)^4}. \tag{24}$$

Boundary condition (3) at the inlet is expressed in terms of the Riemann variables as

$$g(u(0,t),v(0,t)) = Q_{\text{in}}(t) \tag{25}$$

$$g(u,v) = \frac{\rho^2 A_0^2}{4^{\frac{11}{2}}\beta^2}(u+v)(u-v)^4. \tag{26}$$

Together with (20)–(26), we associate a boundary condition at $x = D$, which may be specified as follows.

3) Boundary Condition at the Outlet: Since the 2×2 hyperbolic system (20) and (21) is heterodirectional, together with the boundary condition (25) at $x = 0$, one should specify a boundary condition at $x = D$. There are different options for specifying a boundary condition at $x = D$, also depending on the coupling type, of the arterial segment considered, with different arteries (also considering different types of arteries; see, e.g., [20], [27], [35]).

Since, in this article, we are concentrated on the modeling of bottleneck effects, the boundary condition is specified in order to describe the pressure difference between the locations before and after the bottleneck, also accounting for a cumulative effect of arteries downstream of the stenosis area. This could be achieved employing a static (see Section II-C) or dynamic (see Section II-D) description for the effect of the stenosis. For completeness, we also discuss the case in which there is no stenosis and arteries downstream of the arterial segment considered do not affect its dynamics. In such a case, we explore a nonreflecting (see, e.g., [19], [42]) boundary condition at $x = D$, such that there is no incoming wave at the right boundary. We summarize below these three cases.

1) In the case of static boundary bottleneck, the boundary condition at $x = D$ is specified in order to describe the pressure drop at the outlet of the arterial segment considered, where a stenosis is located, as described in Section II-C. Specifically, using (11), the right boundary condition is expressed in Riemann variables as

$$G(u(D,t),v(D,t)) = 0 \tag{27}$$

where

$$\begin{aligned} G(u,v) = &\rho(u-v)^2 - \frac{32\beta}{\sqrt{A_0}} - d_1(u-v)^4(u+v) \\ &- 4K_s\rho(u+v)^2\left(d_2(u-v)^4 - 1\right)^2 \end{aligned} \tag{28}$$

$$d_1 = \left(R_{\text{T}} + \frac{8\pi\mu L_s}{A_s^2}\right)\frac{\rho^2 A_0^2}{\beta^2 4^3},\quad d_2 = \frac{\rho^2 A_0^2}{4^5\beta^2 A_s}. \tag{29}$$

2) Similarly, in the case of a dynamic boundary bottleneck, the right boundary condition is expressed in Riemann variables using (13) and (18) as

$$v(D,t) = 2X(t) - u(D,t) \tag{30}$$

$$\dot{X}(t) = \frac{1}{32\rho L_s}G(u(D,t),2X(t)-u(D,t)). \tag{31}$$

3) In the case in which there is no stenosis, we explore the option of a nonreflecting, right boundary condition (see, e.g., [19], [42]), such that no incoming wave enters at the right boundary of the arterial segment considered. Such a boundary condition could be compared with a "free" right boundary condition (imposed, e.g., in specific traffic networks, see, e.g., [5], [24]; see also Section III-B). Such a boundary condition could be described as

$$v_t(D,t) = f_1(u(D,t),v(D,t)). \tag{32}$$

In fact, one could observe that, boundary condition (32) implies (for classical solutions) that the Riemann variable corresponding to the negative eigenvalue has zero spatial derivative at the right boundary.

Well-posedness of the 2×2 hyperbolic PDE system (20)–(26) with the dynamic boundary condition (32) [with (24)] or (30) and (31) [with (28)], or the static boundary condition (27) [with (28)] may be guaranteed utilizing, for example, the results in [4] and [31]. To be able to employ such results, certain assumptions are required to be imposed on regularity, size, and compatibility (with boundary conditions) of initial conditions, on size and regularity of flow Q_{in} at the inlet, and on the values of parameters β, A_0, K_s, ρ, L_s, μ, R_{T}, and A_s. Well-posedness of the hyperbolic system considered, for realistic values of the various parameters involved, is also consistent with the dynamic behavior of the actual physical system (see, e.g., [11], [35]). Although important, we do not belabor this issue as it is beyond this article's primary scope.

B. Properties of the Model From a Traffic Flow Perspective

1) The first correspondence with second-order traffic flow models originates in the speed equation (2). Such relation for $K_r = 0$ may be compared to the speed dynamics of Payne–Whitham traffic flow model without the relaxation term (a term that may dictate convergence to a specific equilibrium profile) and with pressure given by (4) (see, e.g., [18], [43], [57]). Equation (1), which expresses the conservation of blood volume entering and exiting an artery segment considered, corresponds to the conservation of the number of vehicles entering and exiting a given highway segment. If $K_r \neq 0$ model (1) and (2) could be also viewed as Payne–Whitham-type with the term $K_r\frac{V}{A}$ playing the role of a type of relaxation term. Nevertheless, in such a case, a fundamental diagram-based reduction, employing the procedure described in

the next paragraph, would not work.[2] We note that both cases may be realistic for blood flow, depending on, for example, whether convection is the dominant effect (thus, simplification $K_r = 0$ may be realistic), see, for example, [11].

2) The correspondence of model (1) and (2) to traffic flow models of Payne–Whitham (and Aw–Rascle–Zhang, see, e.g., [18], [28], [43]) type could be also viewed via a fundamental diagram definition, considering the pressure function (4), which could be explained as follows. Adopting the procedure in [57] for derivation of a fundamental diagram relation from the speed equation (2), we define $V = F(A)$ and substitute this relation into (2) in order to obtain only one, conservation law equation of the form (1), i.e., of the form $A_t + (F(A)A)_x = 0$, where F is to be determined. With $K_r = 0$, we get that

$$F'(A)\left(A_t + F(A)A_x + \frac{\beta}{2\rho A_0\sqrt{A}F'(A)}A_x\right) = 0. \quad (33)$$

Imposing the reasonable requirement that $F'(A) < 0$, for all $A > 0$, relation (33) holds if the following equation is satisfied:

$$A_t + F(A)A_x + \frac{\beta}{2\rho A_0\sqrt{A}F'(A)}A_x = 0. \quad (34)$$

Therefore, in order for (34) to reduce to the conservation law equation (1), imposing $V = F(A)$, for any A, the following should hold:

$$F'(A)^2 = \frac{\beta}{2\rho A_0}A^{-\frac{3}{2}}. \quad (35)$$

Therefore, since $F'(A) < 0$, for any $A > 0$, we get that

$$F(A) = F(0) - 2\sqrt{\frac{2\beta}{\rho A_0}}A^{\frac{1}{4}}. \quad (36)$$

The constant $F(0)$ may be viewed as the speed at a limiting case in which the section area tends to zero. Thus, in practice, it may be defined, for example, through considering a maximum possible, blood transport speed, which could be obtained empirically. Relation (36) defines a fundamental diagram (see, e.g., [43]), satisfying the required conditions. In particular, function $\bar{Q}(A) = AF(A) = A(F(0) - 2\sqrt{\frac{2\beta}{\rho A_0}}A^{\frac{1}{4}})$, for $A \in [0, A_1]$, where $A_1 = \frac{F(0)^4\rho^2A_0^2}{\beta^2 4^3}$, satisfies $\bar{Q}(0) = \bar{Q}(A_1) = 0$, while being strictly concave.

We note here that the limiting case, in which $V = F(A)$, constitutes a considerable simplification, which may appear, at first sight, as not realistic for cardiovascular systems. However, such a reduction may be useful in, for example, studying the dynamic effect of a bottleneck in blood flow, at a vicinity upstream of the stenosis, employing only the respective conservation law equation. Furthermore, introduction, for first time, of the notion of fundamental diagram for cardiovascular flow, could be utilized to characterize, in a computationally tractable and practical manner, the stenosis degree via estimation/quantification of pressure drop magnitude at the stenosis; inspired by respective capacity drop modeling and estimation techniques in traffic flow (via utilization of fundamental diagram for traffic flow) in the presence of bottleneck.

3) The two different bottleneck descriptions also bear a resemblance to traffic flow bottleneck descriptions. For example, boundary bottlenecks may appear due to lane-drops or, in general, due to the presence of locations of reduced capacity, at the end of a controlled area of interest, such as where a tunnel or an area of high curvature begins (see, e.g., [47]). A boundary bottleneck could be described through properly modeling the traffic capacity drop at the bottleneck location (potentially also employing different fundamental diagram relations for the traffic speed immediately before and after the bottleneck location; see, e.g., [43], [55]); corresponding to the static equation (7) [or (10)], which describes the pressure drop at the area of the stenosis that may also be viewed as defining a reduced-pressure fundamental diagram at the stenosis, depending on the pressure immediately before, as $P_s(A, V) = P(A) - V^2\frac{K_s\rho}{2}(\frac{A}{A_s} - 1)^2$ (that becomes a function of only A when $V = F(A)$).

In the case of a dynamic bottleneck description, speed (or flow) dynamics at the area of the stenosis are described by an ODE (as in (13) and (31); see also, e.g., [38], [53]), dictated by the pressure difference between the areas at the inlet and outlet of the stenosis. This may be viewed as corresponding to the case of dynamic description of traffic density at a bottleneck area through an ODE, dictated by the flow difference between the flow arriving and exiting the bottleneck area (see, e.g., [6], [47]). In both cases, the resulting dynamic description consists of a nonlinear, hyperbolic PDE–ODE coupled system.

4) The nonreflecting boundary condition (see, e.g., [19], [42]), considered in the case of no bottleneck, at the outlet of the arterial segment considered, could be compared with a free boundary condition in traffic flow, at the outlet of a highway segment (see, e.g., [5], [24]). Such a boundary condition may describe the fact that the traffic network downstream of a highway segment considered has no effect on the traffic flow dynamics upstream, for example, because there is a capacity increase downstream, e.g., in the case where the right boundary indicates the end of tunnel or end of high curvature. Respectively, in the case of blood flow dynamics such condition is employed to specify the right boundary condition in cases in which the arterial network downstream of the artery segment considered does not have a strong effect in the blood flow inside the domain (for instance, when the downstream blood flow is not obstructed, e.g., by the presence of stenosis), or its effect is difficult, or irrelevant (with respect to modeling the dynamics of the specific artery segment considered) to be modeled. It may be prescribed, for example, as a terminal boundary condition for numerical simulation, see, for example, [17] and [34].

5) For a cardiovascular flow, the subcritical regime is characterized by the sign of $\bar{\lambda}_2$ in (15). Analogously, traffic congestion may be characterized by a negative sign of a respective eigenvalue that corresponds to the Riemann invariant transporting opposite to the traffic flow direction (see, e.g., [7]). One difference lies in that physiological conditions for cardiovascular flow correspond to the subcritical (congested) regime (where $\bar{\lambda}_2 < 0$; see, e.g., [21], [35]), whereas for a traffic flow, physiological conditions may be considered as corresponding to the free-flow (supercritical) regime (where $\bar{\lambda}_2 > 0$; see also, e.g., [7]).

A congested regime is characterized by the sign of $\bar{\lambda}_2$ in (15), irrespectively of the boundary condition considered. In the case of a fundamental diagram-based reduction of the 2×2 hyperbolic PDE model, the condition for congested regime characterization reduces to a condition that the section area A being larger than a critical section area, namely, the point at which the function $AV(A)$ changes monotonicity. In fact, the value of the latter, obtained considering the

[2]For this procedure to be feasible, one would have to modify the corresponding term in (2) to $K_r\frac{F(A)-V}{A}$ [with F given in (36)], such that this term plays the role of relaxation, forcing asymptotic convergence to a specific equilibrium profile. However, whether such a modification is realistic for blood flow would have to be validated, for example, using available data. The reason is that the $K_r\frac{V}{A}$ term is employed to capturing viscous effects of blood flow, whereas the relaxation term dictates convergence to a certain equilibrium profile.

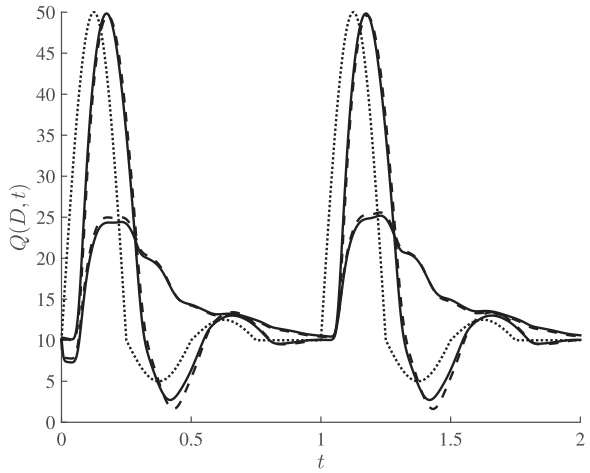

Fig. 2. Dotted line: Inflow $Q_{\rm in}(t)$ to artery segment considered. Solid line: Flow $Q(D,t) = A(D,t)V(D,t)$ at the outlet of a given artery segment using the dynamic bottleneck model (12) for the cases of 75% (corresponding to small values of outflow) and 25% stenosis. Dashed line: Outflow $Q(D,t) = A(D,t)V(D,t)$ using the static bottleneck model (7) for the cases of 75% (corresponding to small values of outflow) and 25% stenosis.

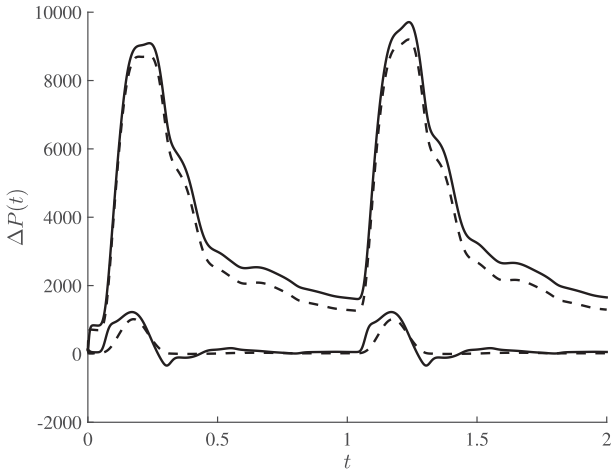

Fig. 3. Pressure drop $\Delta P(t)$ at the stenosis. Solid line: Pressure drop as predicted by the dynamic bottleneck model (12) for the cases of 75% (corresponding to large values of pressure drop) and 25% stenosis. Dashed line: Pressure drop as predicted by the static bottleneck model (7) for the cases of 75% (corresponding to large values of pressure drop) and 25% stenosis.

derived fundamental diagram in (36), namely $\bar{Q}(A) = AF(A)$, would be also consistent with the respective value obtained from (15) [when V is given by (36)] imposing the condition that $\bar{\lambda}_2$ is negative (thus, congested regime characterizations using either of the two descriptions are in alignment).

Even though the blood flow may lie in a congested regime (according to the above characterization), the degree of flow reduction that makes a stenosis to be an actual blood flow bottleneck depends on the magnitude of the pressure drop at the stenosis. The point at which a stenosis pressure drop reduces to a critical point from a clinical viewpoint is crucial. This, in turn, depends on the characteristics of the stenosis and of the given artery, see, for example, [38].

IV. Numerical Simulation of the Stenosis Model and Its Usefulness for Adaptive Observer Design

A. Simulation of Static/Dynamic Boundary Bottleneck Models

We present simulation examples of the dynamic and static bottleneck formulations. We choose a numerical example with realistic values for the parameters (see, e.g., [21], [38], [53]). Specifically, as regards (2), we choose $D = 10$, $\rho = 1$, and $K_r = 8\pi\nu = 8\pi \times 0.035$. As regards the pressure function (4), we set $b = \frac{4}{3}$, $h = 0.05$, $E = 3 \times 10^5$, and $A_0 = \pi \times 0.5^2$. For the right boundary condition, we set $R_{\rm T} = 100$ and $K_{\rm s} = 1.5$. We solve numerically, employing a finite-difference scheme with discrete time and spatial steps equal to 10^{-4} and 0.4, respectively, the system in Riemann coordinates, i.e., (20) and (21), recovering the numerical solution in the original variables via (18) and (19). The initial conditions for u and v are chosen as constant for simplicity. They are given by (16) and (17), with $V_{\rm initial}(x) = \frac{Q_{\rm in}(0)}{A_{\rm initial}(x)}$ and $A_{\rm initial}(x) = (\sqrt{A_0} + R_{\rm T}Q_{\rm in}(0)\frac{A_0}{\beta} + \frac{A_0 K_{\rm s}\rho}{2\beta}Q_{\rm in}(0)^2(\frac{2}{A_0} - \frac{1}{A_0})^2)^2$.

For the left boundary condition (25) and (26) we specify the inflow $Q_{\rm in}$ shown in Fig. 2 (dotted line), having, qualitatively, a simple, nevertheless realistic form with respect to blood flow shape (see, e.g., [21], [38], [53]). For the right boundary condition, we consider two cases. The static boundary condition case in which we employ (27) and (28) with $L_{\rm s} = 0$ and the dynamic boundary condition case in which we employ (30) and (31) [where an Euler scheme is employed for solving (31) numerically] with $\mu = 0.045$ and $L_{\rm s} = \frac{D}{10}$. For each of the two cases, we consider two different stenosis areas, one with $\frac{A_{\rm s}}{A_0} = 0.25$ (corresponding to a 75% stenosis) and one with $\frac{A_{\rm s}}{A_0} = 0.75$ (corresponding to a 25% stenosis). In Fig. 2, we show the respective numerical solutions for the outflow $Q(D,t) = A(D,t)V(D,t)$. In Fig. 3, we show the pressure drop, as predicted by (7) for the static boundary case and as predicted by solving (12) with respect to ΔP for the dynamic boundary case, for the four cases. Pressure drop increases with an increase in stenosis severity, i.e., with a decrease of the area $A_{\rm s}$. In the case of dynamic boundary, larger values of pressure drop are observed, which is explained in view of the fact that the length of stenosis and potential blood acceleration due to the stenosis (see, e.g., [53]) are also accounted for [via (12)].

B. Models Formulation Toward Adaptive Observer Design

The uncertain parameters are related to the characteristics of the stenosis. The rest of the parameters involved in the model, for example, related to blood flow properties, can be empirically/experimentally identified, and thus, could be considered as known (see, e.g., [38], [52], [53]). Thus, the uncertain parameters are the location D, the length $L_{\rm s}$, and the section area $A_{\rm s}$ of the stenotic region. These parameters appear at the right boundary and the characteristic speeds, which can be seen as follows. We first rescale the domain length in order to move the uncertainty in the domain length to an uncertainty in the characteristic speeds (that would allow a linear parameterization of the uncertain parameter, at least in the case where the full state was measured). This can be seen defining $z = \frac{x}{D}$ and rewriting (20) and (21) as

$$\begin{aligned}\bar{u}_t(z,t) = &-\theta_1\lambda_1\left(\bar{u}(z,t),\bar{v}(z,t)\right)\bar{u}_z(z,t)\\ &+ f_1\left(\bar{u}(z,t),\bar{v}(z,t)\right) \qquad (37)\\ \bar{v}_t(z,t) = &-\theta_1\lambda_2\left(\bar{u}(z,t),\bar{v}(z,t)\right)\bar{v}_z(z,t)\\ &+ f_1\left(\bar{u}(z,t),\bar{v}(z,t)\right) \qquad (38)\end{aligned}$$

where $\theta_1 = \frac{1}{D}$, $z \in [0,1]$, $\bar{u}(z) = u(zD)$, and $\bar{v}(z) = v(zD)$. The left boundary condition (25) incorporates no uncertain parameter, while the

available measurements are now $\bar{v}(0)$ and $\bar{u}(0)$. The right boundary condition (27)–(29) or (30) and (31) incorporates the uncertain parameters $L_{\rm s}$ and $A_{\rm s}$.

When it is assumed that $L_{\rm s}$ is very small, one could formulate a simultaneous state estimation and parameters identification problem in a tractable manner as follows. Manipulating boundary condition (27), we get (as long as $A_{\rm s} < A(D)$)

$$\bar{G}\left(\bar{u}(1), \bar{v}(1)\right) = \theta_2 \tag{39}$$

where $\bar{G}(\bar{u}, \bar{v}) = 4^5\beta^2 \frac{\sqrt{\frac{\rho(\bar{u}-\bar{v})^2 - \frac{32\beta}{\sqrt{A_0}} - d_1(\bar{u}-\bar{v})^4(\bar{u}+\bar{v})}{4K_{\rm s}\rho(\bar{u}+\bar{v})^2}} + 1}{\rho^2 A_0^2(\bar{u}-\bar{v})^4}$, $\theta_2 = \frac{1}{A_{\rm s}}$. A system consisting of (37)–(39) and (25) could be utilized for designing an adaptive observer, toward simultaneous state and parameters estimation. Although we are not aware of a result presenting such a design, we will pursue this in our future research, also drawing inspiration by the designs for general, linear hyperbolic systems and traffic flows; see, for example, [1], [2], [9], [48] and [37], [54], respectively, for performing such a design for a potentially linearized version. Even for a linearized version, the main technical challenges for designing an adaptive observer stem from (in addition to the linearized hyperbolic system being time-varying, as typical, reference blood inflow to a given artery segment is time-varying, thus generating a time-varying reference trajectory) the simultaneous presence of unknown transport speeds (since the full state is not measured) and unknown boundary parameters at the boundary anticollocated with the boundary where measurements are available. These challenges make it difficult, for example, to transform (even a linearized version of) system (37)–(39), and (25) with boundary measurements at $z = 0$ in a canonical form suitable for adaptive observer design.

Similarly, for the more complex case in which the dynamic boundary condition (30) and (31) is employed, one could formulate the problem as a problem of simultaneous state and parameters estimation for a respective PDE–ODE coupled system, consisting of (37), (38), (25), and the boundary condition (30), with unknown parameters $\theta_1 = \frac{1}{D}$, $\theta_2 = \frac{1}{A_{\rm s}}$, and $\theta_3 = \frac{1}{L_{\rm s}}$.

V. Conclusion and Discussion

The arterial stenosis models presented and the correspondence with vehicular traffic flow bottleneck models may constitute the starting point for PDE-based, control-theoretic developments for cardiovascular flow stenosis analysis, estimation, and control, inspired by respective traffic flow techniques.

A crucial issue for addressing the feedback control problem of blood flow at areas with stenosis would be to specify how, in practice, the required actuation could be performed. One possibility would be to consider boundary actuation, manipulating the inflow in (25) through certain micro-electromechanical systems (e.g., smart stent/shunt devices, actuated wirelessly; see, e.g., [12], [41], [50]), thus resulting in a boundary control problem for system (20), (21), and (25) with either (27) or (30), (31). An alternative possibility would be to consider in-domain actuation enabled through automated drug delivery systems (see, e.g., [12], [49]). Such an approach could build upon an extension of the presented model to incorporate in-domain actuation, in correspondence with automated vehicles-based actuation incorporation in vehicular traffic (see, e.g., [5], [16], [25], [33], [51]). Accordingly, the stability of the PDE models presented should be also studied (even in an open loop).

Acknowledgment

The author would like to thank Prof. Argiris Delis and Prof. Ioannis Nikolos for fruitful discussions.

References

[1] H. Anfinsen and O. M. Aamo, "Estimation of parameters in a class of hyperbolic systems with uncertain transport speeds," in *Proc. Mediterranean Conf. Control Automat.*, 2017, pp. 80–87.
[2] H. Anfinsen and O. M. Aamo, *Adaptive Control of Hyperbolic PDEs*. Berlin, Germany: Springer, 2019.
[3] J. Auriol and F. D. Meglio, "Robust output feedback stabilization for two heterodirectional linear coupled hyperbolic PDEs," *Automatica*, vol. 115, 2020, Art. no. 108896.
[4] G. Bastin and J.-M. Coron, *Stability and Boundary Stabilization of 1-D Hyperbolic Systems*. Basel, Switzerland: Birkhäuser, 2016.
[5] N. Bekiaris-Liberis and A. Delis, "PDE-based feedback control of freeway traffic flow via time-gap manipulation of ACC-equipped vehicles," *IEEE Trans. Control Syst. Technol.*, vol. 29, no. 1, pp. 461–469, Jan. 2021.
[6] N. Bekiaris-Liberis and M. Krstic, "Compensation of actuator dynamics governed by quasilinear hyperbolic PDEs," *Automatica*, vol. 92, pp. 29–40, 2018.
[7] F. Belletti, M. Huo, X. Litrico, and A. M. Bayen, "Prediction of traffic convective instability with spectral analysis of the Aw–Rascle–Zhang model," *Phys. Lett. A*, vol. 379, pp. 2319–2330, 2015.
[8] V. Bikia, "Non-invasive monitoring of key hemodynamical and cardiac parameters using physics-based modelling and artificial intelligence," Ph.D. dissertation, Inst. Bioeng., EPFL, Lausanne, Switzerland, 2021.
[9] M. Bin and F. D. Meglio, "Boundary estimation of boundary parameters for linear hyperbolic PDEs," *IEEE Trans. Autom. Control*, vol. 62, no. 8, pp. 3890–3904, Aug. 2017.
[10] S. Blandin, X. Litrico, M. L. D. Monache, B. Piccoli, and A. Bayen, "Regularity and Lyapunov stabilization of weak entropy solutions to scalar conservation laws," *IEEE Trans. Autom. Control*, vol. 62, no. 4, pp. 1620–1635, Apr. 2017.
[11] S. Canic and E. H. Kim, "Mathematical analysis of the quasilinear effects in a hyperbolic model blood flow through compliant axi-symmetric vessels," *Math. Methods Appl. Sci.*, vol. 26, pp. 1161–1186, 2003.
[12] F. A. M. Chazali, M. N. Hasan, T. Rehman, M. Nafea, M. S. M. Ali, and K. Takahata, "MEMS actuators for biomedical applications: A review," *J. Micromechanics Microengineering*, vol. 30, 2020, Art. no. 073001.
[13] X. Chen, B. Assadsangabi, Y. Hsiang, and K. Takahata, "Enabling angioplasty-ready 'Smart' stents to detect in-stent restenosis and occlusion," *Adv. Sci.*, vol. 5, 2018, Art. no. 1700560.
[14] C. Clark, "The fluid mechanics of aortic stenosis–I. Theory and steady flow experiments," *J. Biomech.*, vol. 9, pp. 521–528, 1976.
[15] C. Claudel and A. Bayen, "Lax–Hopf based incorporation of internal boundary conditions into Hamilton–Jacobi equation–Part I: Theory," *IEEE Trans. Autom. Control*, vol. 55, no. 5, pp. 1142–1157, May 2010.
[16] S. Darbha and K. R. Rajagopal, "Intelligent cruise control systems and traffic flow stability," *Transp. Res. C*, vol. 7, pp. 329–352, 1999.
[17] M. L. D. Monache, B. Piccoli, and F. Rossi, "Traffic regulation via controlled speed limit," *SIAM J. Control Optim.*, vol. 55, pp. 2936–2958, 2017.
[18] S. Fan, M. Herty, and B. Seibold, "Comparative model accuracy of a data-fitted generalized Aw–Rascle–Zhang model," *Netw. Heterogenous Media*, vol. 9, pp. 239–268, 2014.
[19] L. Formaggia, D. Lamponi, and A. Quarteroni, "One dimensional models for blood flow in arteries," *J. Eng. Math.*, vol. 47, pp. 251–276, 2003.
[20] L. Formaggia, D. Lamponi, M. Tuveri, and A. Veneziani, "Numerical modeling of 1D arterial networks coupled with a lumped parameters description of the heart," *Comput. Methods Biomech. Biomed. Eng.*, vol. 9, pp. 273–288, 2006.
[21] L. Formaggia, F. Nobile, and A. Quarteroni, "A one dimensional model for blood flow: Application to vascular prosthesis," in *Mathematical Modeling and Numerical Simulation in Continuum Mechanics*, vol. 19, I. Babuska, T. Miyoshi, and P. G. Ciarlet, Eds., Berlin, Germany: Springer, 2002, pp. 137–153.
[22] P. Goatin, S. Gottlich, and O. Kolb, "Speed limit and ramp meter control for traffic flow networks," *Eng. Optim.*, vol. 48, pp. 1121–1144, 2016.
[23] L. Hu, F. D. Meglio, R. Vazquez, and M. Krstic, "Control of homodirectional and general heterodirectional linear coupled hyperbolic PDEs," *IEEE Trans. Autom. Control*, vol. 61, no. 11, pp. 3301–3314, Nov. 2015.

[24] I. Karafyllis, N. Bekiaris-Liberis, and M. Papageorgiou, "Feedback control of nonlinear hyperbolic PDE systems inspired by traffic flow models," *IEEE Trans. Autom. Control*, vol. 64, no. 9, pp. 3647–3662, Sep. 2019.
[25] I. Karafyllis, D. Theodosis, and M. Papageorgiou, "Analysis and control of a non-local PDE traffic flow model," *Int. J. Control*, vol. 95, pp. 660–678, 2022.
[26] A. Kiourti and K. S. Nikita, "A review of in-body biotelemetry devices: Implantables, ingestibles, and injectables," *IEEE Trans. Biomed. Eng.*, vol. 64, no. 7, pp. 1422–1430, Jul. 2017.
[27] T. Koeppl, G. Santin, B. Haasdonk, and R. Helmig, "Numerical modelling of a peripheral arterial stenosis using dimensionally reduced models and kernel methods," *Numer. Methods Biomed. Eng.*, vol. 34, 2018, Art. no. e3095.
[28] J.-P. Lebacque, S. Mammar, and H. Haj-Salem, "The Aw–Rascle and Zhang's model: Vacuum problems, existence and regularity of the solutions of the Riemann problem," *Transp. Res. Part B: Methodological*, vol. 41, pp. 710–721, 2007.
[29] K. W. Lee and X. Y. Xu, "Modelling of flow and wall behaviour in a mildly stenosed tube," *Med. Engin. Phys.*, vol. 24, pp. 575–586, 2002.
[30] T. Li and S. Canic, "Critical thresholds in a quasilinear hyperbolic model of blood flow," *Netw. Heterogen. Media*, vol. 4, pp. 527–536, 2009.
[31] T.-T. Li, *Global Classical Solutions for Quasilinear Hyperbolic Systems*. Hoboken, NJ, USA: Wiley, 1994.
[32] J. C. Misra and S. Chakravarty, "Flow in arteries in the presence of stenosis," *J. Biomech.*, vol. 19, pp. 907–918, 1986.
[33] G. Piacentini, P. Goatin, and A. Ferrara, "Traffic control via platoons of intelligent vehicles for saving fuel consumption in freeway systems," *IEEE Control Syst. Lett.*, vol. 5, no. 2, pp. 593–598, Apr. 2021.
[34] A. Quarteroni, L. Dede, A. Manzoni, and C. Vergara, *Mathematical Modelling of the Human Cardiovascular System: Data, Numerical Approximation, Clinical Applications*, Cambridge, U.K.: Cambridge Univ. Press, 2019.
[35] A. Quarteroni and L. Formaggia, "Mathematical modelling and numerical simulation of the cardiovascular system," in *Handbook of Numerical Analysis*, vol. 12, N. Ayache, Ed., Amsterdam, The Netherlands: Elsevier, 2004, pp. 3–127.
[36] B. D. Seeley and D. F. Young, "Effect of geometry on pressure losses across models of arterial stenoses," *J. Biomech.*, vol. 9, pp. 439–448, 1976.
[37] T. Seo, A. M. Bayen, T. Kusakabe, and Y. Asakura, "Traffic state estimation on highway: A comprehensive survey," *Annu. Rev. Control*, vol. 43, pp. 128–151, 2017.
[38] N. Stergiopulos, D. F. Young, and T. R. Rogge, "Computer simulation of arterial flow with applications to arterial and aortic stenosis," *J. Biomech.*, vol. 25, pp. 1477–1488, 1992.
[39] K. Takahata, Y. B. Gianchandani, and K. D. Wise, "Micromachined antenna stents and cuffs for monitoring intraluminal pressure and flow," *J. Microelectromech. Syst.*, vol. 15, pp. 1289–1298, 2006.
[40] K. Takashima, T. Kitou, K. Mori, and K. Ikeuchi, "Simulation and experimental observation of contact conditions between stents and artery models," *Med. Eng. Phys.*, vol. 29, pp. 326–335, 2007.
[41] Y. Tal, "Device and method for regulating blood flow," US Patent no. 7.476.200 B2, Jan. 13, 2009.
[42] K. W. Thompson, "Time dependent boundary conditions for hyperbolic systems," *J. Comput. Phys.*, vol. 68, pp. 1–24, 1987.
[43] M. Treiber and A. Kesting, *Traffic Flow Dynamics: Data, Models and Simulation*. Berlin, Germany: Springer, 2013.
[44] L. Tumash, C. C. de Wit, and M. L. D. Monache, "Boundary control design for traffic with nonlinear dynamics," *IEEE Trans. Autom. Control*, vol. 67, no. 3, pp. 1301–1313, Mar. 2022.
[45] L. Tumash, C. C. de Wit, and M. L. D. Monache, "Boundary control for multi-directional traffic on urban networks," in *Proc. IEEE Conf. Decis. Control*, 2021, pp. 2671–2676.
[46] X. Wang, " 1D modeling of blood flow in networks: Numerical computing and applications," Ph.D. dissertation, Univ. Pierre and Marie Curie, Paris, France, 2014.
[47] Y. Wang, E. B. Kosmatopoulos, M. Papageorgiou, and I. Papamichail, "Local ramp metering in the presence of a distant downstream bottleneck: Theoretical analysis and simulation study," *IEEE Trans. Intell. Transp. Syst.*, vol. 15, no. 5, pp. 2024–2039, Oct. 2014.
[48] J. Wang and M. Krstic, "Regulation-triggered adaptive control of hyperbolic PDE-ODE model with boundary interconnections," *Int. J. Adaptive Control Signal Process.*, vol. 35, pp. 1513–1543, 2021.
[49] G.-Z. Yang, Ed., *Body Sensor Networks*. London, U.K.: Springer, 2014.
[50] Y. Yi, J. Chen, and K. Takahata, "Wirelessly powered resonant-heating stent system: Design, prototyping, and optimization," *IEEE Trans. Antennas Propag.*, vol. 68, no. 1, pp. 482–490, Jan. 2020.
[51] J. Yi and R. Horowitz, "Macroscopic traffic flow propagation stability for adaptive cruise controlled vehicles," *Transp. Res. C, Emerg. Technol.*, vol. 14, pp. 81–95, 2006.
[52] D. F. Young and F. Y. Tsai, "Flow characteristics in models of arterial stenoses–I. Steady flow," *J. Biomech.*, vol. 6, pp. 395–410, 1973.
[53] D. F. Young and F. Y. Tsai, "Flow characteristics in models of arterial stenoses–II. Unsteady flow," *J. Biomech.*, vol. 6, pp. 547–559, 1973.
[54] H. Yu, Q.-J. Gan, A. Bayen, and M. Krstic, "PDE traffic observer validated on freeway data," *IEEE Trans. Control Syst. Technol.*, vol. 29, no. 3, pp. 1048–1060, May 2021.
[55] H. Yu, S. Koga, T. R. Oliveira, and M. Krstic, "Extremum seeking for traffic congestion control with a downstream bottleneck," *ASME J. Dyn. Syst., Measur., Control*, vol. 143, 2021, Art. no. 031007.
[56] H. Yu and M. Krstic, "Traffic congestion control of Aw–Rascle–Zhang model," *Automatica*, vol. 100, pp. 38–51, 2019.
[57] H. M. Zhang, "A non-equilibrium traffic model devoid of gas-like behavior," *Transp. Res. Part B*, vol. 36, pp. 275–290, 2002.
[58] L. Zhang, C. Prieur, and J. Qiao, "PI boundary control of linear hyperbolic balance laws with stabilization of ARZ traffic flow models," *Syst. Control Lett.*, vol. 123, pp. 85–91, 2019.